applied sciences

MDPI

*Communication*

# Hyperthermia Efficiency of Magnetic Nanoparticles in Dense Aggregates of Cerium Oxide/Iron Oxide Nanoparticles

**Cindy Yadel [1], Aude Michel [1], Sandra Casale [2] and Jerome Fresnais [1,*]**

[1] Laboratoire de Physico-Chimie des Electrolytes et Nanosystèmes Interfaciaux, PHENIX, UMR 8234, CNRS, Sorbonne Université, F-75252 Paris CEDEX 05, France; cindy.yadel@gmail.com (C.Y.); aude.michel@upmc.fr (A.M.)

[2] Service de Microscopie Electronique de l'UFR de Chimie Paris VI, 4 Place Jussieu, 75252 Paris CEDEX 05, France; sandra.casale@sorbonne-universite.fr

* Correspondence: jerome.fresnais@sorbonne-universite.fr; Tel.: +33-(0)1-4427-4309

Received: 13 July 2018; Accepted: 25 July 2018; Published: 27 July 2018


**Featured Application: Magnetic hyperthermia applications suffer from a dramatic decrease of efficiency when nanoparticles aggregate. By combining magnetic and non-magnetic nanoparticles into nanostructured systems, it is possible to recover mainly the initial heating efficiency.**

**Abstract:** Iron oxide nanoparticles are intended to be used in bio-applications for drug delivery associated with hyperthermia. However, their interactions with complex media often induces aggregation, and thus a detrimental decrease of their heating efficiency. We have investigated the role of iron oxide nanoparticles dispersion into dense aggregates composed with magnetic/non-magnetic nanoparticles and showed that, when iron oxide nanoparticles were well-distributed into the aggregates, the specific absorption rate reached 79% of the value measured for the well-dispersed case. This study should have a strong impact on the applications of magnetic nanoparticles into nanostructured materials for therapy or catalysis applications.

**Keywords:** magnetic nanoparticle; hyperthermia; aggregation; dipolar interactions

## 1. Introduction

Magnetic hyperthermia is a powerful technique envisaged to heat up materials or tissues. Used as probes for cancer therapy, iron oxide nanoparticles are largely studied coupled to hyperthermia to activate cell death [1] or molecular release. Iron oxide nanoparticles are non-toxic [2], and eliminated by the cells in vivo [3]. However, the heating properties of iron oxide nanoparticles are often deteriorated by their aggregation [1,4]. This involves a drastic decrease of the specific loss power (SLP, or SAR in some publication, for specific absorption rate), which corresponds to the heat energy loss by the particles toward their environment [5]. Recovering high SLP values during application is really important because this normalized value is the one that is used to compare the efficiency of iron oxide nanoparticles directly depending on their synthesis procedure. Optimized nanoparticles excited with the right frequencies demonstrate large SLP values (see, for instance, the work of Fortin et al. [6]). When specific synthesis pathways are used, large SLP values can be obtained [7]. Thus, aggregation is the main drawback that hamper the recent improvements in nanoparticle synthesis pathways. As a consequence, this drastically limits their applicability or necessitates a larger nanoparticle amount to produce the expected macroscopic thermal effect. Against this macroscopic effect, some groups already showed that magnetic hyperthermia could be useful in close proximity of the nanoparticles [8–11]. This is true for well-dispersed stable nanoparticles, but could also be applied to nanostructured

materials containing iron oxide material as local heating sources. To avoid detrimental interparticle dipolar interactions, it is necessary to tune the mean distance between magnetic nanoparticles inside nanostructured materials. However, this point is most always forgotten, or indirectly established by regarding the heating effect (either structure change or release ability) on the nanostructured systems. In this article, we investigated the role of dipolar interaction of maghemite nanoparticles embedded into aggregates between non-magnetic and magnetic nanoparticles with similar sizes. We thus wondered how to tune the interparticle dipolar interactions between magnetic nanoparticles into aggregates, to reach highly efficient nanostructured materials with embedded magnetic nanoparticles. To tune the mean distance between $Fe_2O_3$ nanoparticles, we investigated their heating efficiency when aggregated with non-magnetic cerium oxide nanoparticles. They were selected because they exhibit similar surface chemistry reactivity and present the same dependence of the surface charges versus pH values. To ensure a homogeneous distribution into the aggregates, we selected an aggregation pathway that introduced a non-directed link between nanoparticles through electrostatic interactions with an oppositely charged polyelectrolyte.

## 2. Materials and Methods

Iron oxide nanoparticles were synthesized by soft chemistry methods, according to the so-called "Massart" pathway through the nanoprecipitation of Fe(II) and Fe(III) ions in a basic medium (VWR, Fontenay-sous-Bois, France), followed by an oxidation of the magnetite into maghemite [12]. Nanoparticles had a mean diameter of 7 nm and a polydispersity following a lognormal law of 0.4. An already published size sorting process was applied to the sample to obtain 10.6 $\pm$ 6.2 nm large nanoparticles with a narrower size polydispersity [13]. The principle is based on the phase separation of the particles by tuning the balance between attractive (magnetic attraction together with Van Der Waals) and repulsive (surface charges) forces that are governed by the size of the particles. Nitric acid (playing the role of a salt) is added in a controlled manner to induce a phase separation between concentrated droplets containing the largest particles and the main phase containing the smallest particles. Typically, 5 mL of $HNO_3$ at 8.3 mol·$L^{-1}$ (VWR, Fontenay-sous-Bois, France) was added to 1 L of ferrofluid. The beaker was placed on a magnet and the supernatant (S) was removed. The precipitate phase (C) was washed with acetone (three folds) and diethyl ether (three folds) and redispersed in distilled water. $HNO_3$ was added to the supernatant and the same process was repeated until the final supernatant remained clear from nanoparticles.

Cerium oxide nanoparticles were also synthesized by a soft chemistry process using cerium nitrate solution in a basic medium [14]. Cerium oxide nanoparticles were used as-synthesized without further size sorting. Their mean diameter corresponded to 7.8 $\pm$ 5.2 nm. Both particle types were coated with poly(acrylic acid) polymers with molecular weight of 2100 g/mol (denoted PAA in the rest of the document, Sigma Aldrich, Darmstadt, Germany) to ensure a good colloidal stability as well as to introduce a large amount of negative charges for the following electrostatic interaction with the positive polyelectrolyte [15]. Figure 1 represents the transmission electron microscope (TEM) images of PAA-$CeO_2$ and PAA-$Fe_2O_3$ nanoparticles and their size distribution with a Gaussian fit.

Additionally, PAA-$CeO_2$ and PAA-$Fe_2O_3$ particles were dialyzed to remove the residual free PAA chains put in excess during the coating to ensure a complete coating of both iron oxide and cerium oxide nanoparticles. Poly(trimethylammoniumethylacrylate)-b-poly(acrylamide) block copolymers were synthesized by Madix® controlled radical polymerization [16]. The copolymer was abbreviated $PTEA_{11K}$-b-$PAM_{30K}$, where the indices indicate the molecular weights targeted by the synthesis. The role of the poly(acrylamide) block is preponderant because it will ensure a steric repulsion between aggregates, thus allowing a good colloidal and structural stability against sedimentation that is mandatory to obtain highly concentrated samples for hyperthermia evaluation.

Dispersion of PAA-$CeO_2$, PAA-$Fe_2O_3$, and $PTEA_{11K}$-b-$PAM_{30K}$ copolymer solution were prepared at 0.5 wt % and with 0.5 M $NH_4Cl$. We varied the proportion $r$ of $Fe_2O_3/CeO_2$ from 1.5 to 0.17 and always kept the ratio of nanoparticles/polymer equal to 0.5 to ensure an excess of the complexing

$PTEA_{11K}$-b-$PAM_{30K}$. Results obtained with a mixture of both particles were compared to iron oxide nanoparticles only, aggregated with the same pathway. As demonstrated in our previous work, a dilution from 0.5 M $NH_4Cl$ to 0.1 M $NH_4Cl$ allowed for the formation of aggregates [17–19].

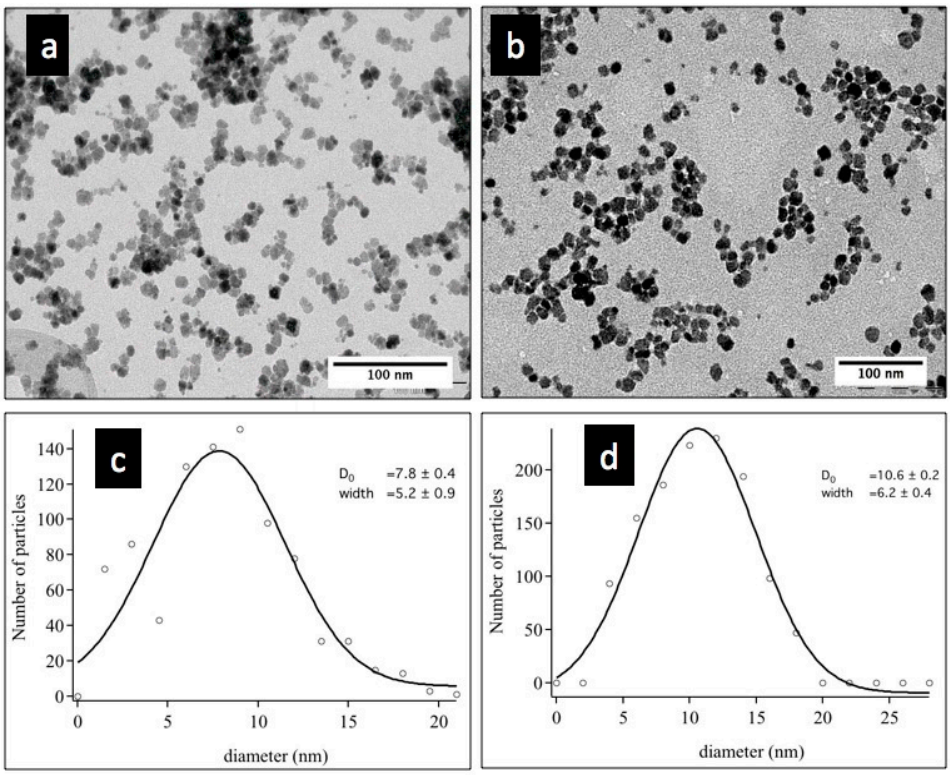


**Figure 1.** Transmission electron microscope (TEM) images of PAA-$CeO_2$ (**a**) and PAA-$Fe_2O_3$ (**b**) nanoparticles. Statistical analysis of TEM images to determine the mean diameter of PAA-$CeO_2$ (**c**) and PAA-$Fe_2O_3$ (**d**) with a Gaussian fit.

Samples were centrifuged and the supernatant was eliminated to access a higher concentration of iron oxide nanoparticles in the final samples in the range of 0.1–0.5 wt % to ensure a measurable temperature increase during hyperthermia analysis.

Dynamic light scattering was performed with a Malvern NanoZS (wavelength $\lambda$ = 656 nm, scattering angle $\theta = 173°$, Malvern Instruments Ltd., Malvern, UK). TEM images were recorded using a JEOL 2010 $LaB_6$ 200kV (TSS Microscopy, Beaverton, OR, USA) microscope, thanks to the microscopy platform at Sorbonne University, Paris, France.

Specific loss power (SLP) was determined using a commercial apparatus from magneTherm (nanoTherics Ltd., Newcastle under Lyme, Staffordshire, UK), alternating magnetic field at 335 kHz with a magnetic field amplitude of 7 mT). To analyze the curve representing the increase of the temperature versus the time, we used an exponential fit, also known as the Box-Lucas method, to take into account the non-adiabatic regime of the increase of temperature during magnetic excitation [20]. In this case, the increase of temperature is fitted using Equation (1).

$$T - T_0 = A(1 - e^{-\lambda(t+t_0)}) \quad (1)$$

where $A$ and $\lambda$ are constants, $t_0$ correspond to the switching on of the magnetic excitation. The SLP value is thus obtained following the Equation (2).

$$SLP = A\lambda C_p / m_{MNP} \quad (2)$$

where *Cp* corresponds to the thermal capacity of the solvent and $m_{MNP}$ is the mass of magnetic nanoparticles per 100 g of magnetic material.

## 3. Results and Discussion

Iron oxide nanoparticles are very efficient hyperthermia probes, but their efficiency drops when aggregated [1,4]. To avoid detrimental dipolar interaction in nanostructured systems, we mixed iron oxide nanoparticles with non-magnetic cerium oxide ones. Both particle types were synthesized and coated with respect to the existing procedures described in materials and methods. PAA-coated nanoparticles exhibit particular good colloidal stability in various complex media such as brine solutions, ionic liquids, or cell culture media [17,21,22].

In particular, we demonstrated in our previous work that it was possible to avoid the aggregation of PAA-coated nanoparticles and positive polyelectrolytes by the addition of salt and allow the aggregation by dilution or dialysis [17,19]. It was achieved for iron oxide or cerium oxide nanoparticles coated with PAA, separately. The present work is dedicated to the co-assembly of iron oxide and cerium oxide nanoparticles into aggregates that could be a model for iron oxide nanoparticles diluted into nanostructured matrices. The objective was to highlight the role of dipolar interaction when nanoparticles are immobilized in aggregates. We chose to use electrostatic complexation because the interactions were conducted between both types of nanoparticles and the positives polyelectrolytes. The process engaged in the complexation did not depend on the nature of the inorganic core of the particles, but only on the interactions between PAA chains and the positive polyelectrolyte ones.

As a confirmation, Figure 2 shows the hydrodynamic diameter of the mixture between iron oxide, cerium oxide, and a 1:1 mixture of both particles with $PTEA_{11K}$-b-$PAM_{30K}$ versus the $NH_4Cl$ concentration. When dispersions of nanoparticles at 0.5 M $NH_4Cl$ of PAA-$Fe_2O_3$, PAA-$CeO_2$, and a mixture of PAA-$Fe_2O_3$ and PAA-$CeO_2$ in the ratio 1:1 with $PTEA_{11K}$-b-$PAM_{30K}$ were diluted with water, the aggregation state occurred at the same critical $NH_4Cl$ concentration. From 0.5 M down to 0.38 M $NH_4Cl$, nanoparticles were well-dispersed and the hydrodynamic diameter corresponded only to the ones of the particles. For a $NH_4Cl$ concentration lower than 0.38 M, the diameters of the objects in solution increased, demonstrating the aggregation through electrostatic interactions.

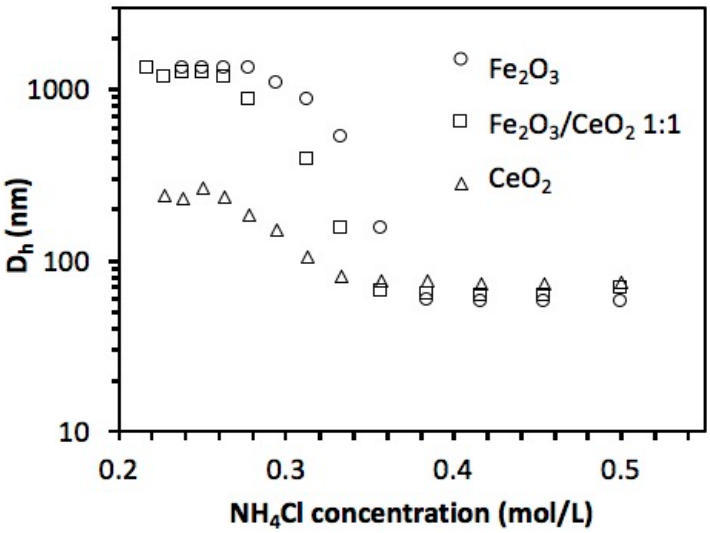


**Figure 2.** Hydrodynamic diameter versus ionic strength for mixture of $PTEA_{11K}$-b-$PAM_{30K}$ with $Fe_2O_3$ (circles), $CeO_2$ (triangles), and a mixture of $Fe_2O_3$ and $CeO_2$ (squares) with the ratio 1:1.

The aggregation occurred at the same salt concentration for both particles and their mixtures, which allowed for the formation of assemblies containing the two particle types. This was confirmed by electron energy loss spectroscopy (EELS) analysis on TEM microscope. We showed a uniform

repartition of both iron oxide and cerium oxide nanoparticles in the aggregates (Figure 3). Furthermore, the ratio between cerium and iron particles in the aggregate corresponded to 67.5% and 32.5%, respectively. This is in good agreement with the introduced ratios in the mixture in brine (16.7% of PAA-$Fe_2O_3$ and 83.3% of PAA-$CeO_2$). The second ratio is due to the stoichiometry of maghemite compared to the one of cerium oxide nanoparticles.

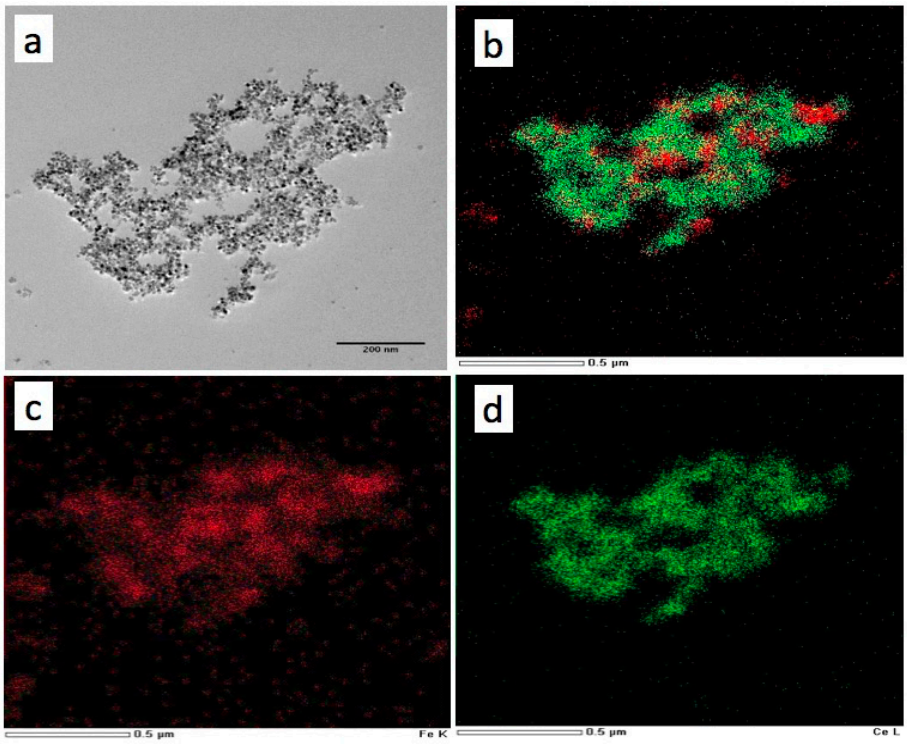


**Figure 3.** (**a**) TEM image of an aggregate of $Fe_2O_3$ and $CeO_2$ NPs; (**b**) Electron energy loss spectroscopy (EELS) analysis of Fe (red) and Ce (green) in the aggregates; (**c**) separated EELS map of the Fe (red) content; (**d**) separated EELS map of the Ce (green) content.

The SLP was measured for well dispersed iron oxide and cerium oxide nanoparticles. Complementarily, aggregated samples containing increasing concentrations of iron oxide ($Fe_2O_3/CeO_2$ ratios from 0.17 to 1.5) were stimulated under an alternative magnetic field. Figure 4 represents the variation of temperature of the samples submitted to an alternative magnetic field. Magnetic field was applied after 60 s of recording of the temperature to ensure that the temperature was stable. There was some variation in iron oxide concentration from one sample to another. For instance, well-dispersed SLP was measured at 0.67 wt % (Figure 4A). In this case, an increase of temperature of 0.8 °C was achieved within 40 s.

SLP measurement for aggregates containing 17% iron oxide nanoparticles (and 83% cerium oxide) was conducted with an MNP concentration of 0.22 wt % (Figure 4C). An increase of 0.5 °C was obtained after the application of the magnetic field for 60 s.

For aggregates made of 100% iron oxide nanoparticles, the SLP measurements were achieved at 0.24 wt % (Figure 4D). For this sample, the increase of temperature up to 0.4 °C was only obtained for 120 s of excitation.

As attended, the temperature of cerium oxide nanoparticles did not increase while alternative magnetic field is on (Figure 4B).

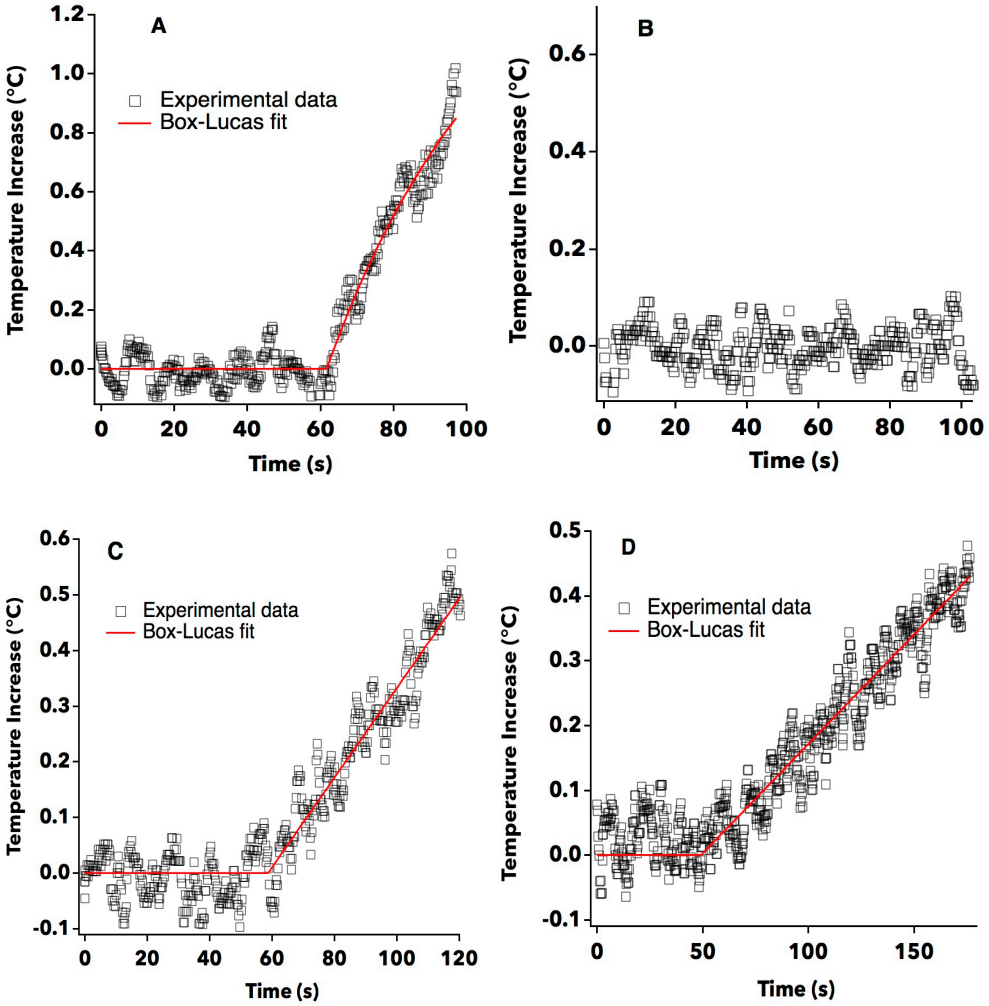


**Figure 4.** Temperature increase and Box-Lucas fit (red line) versus time for well dispersed MNPs (**A**), cerium oxide nanoparticles (**B**), and aggregates containing 17% (**C**) and 100% (**D**) of iron oxide nanoparticles, respectively. Magnetic field was applied after 60 s recording.

By changing the ratio of PAA-$Fe_2O_3$ and PAA-$CeO_2$ particles in the salted mixture from 100 (arbitrary value corresponding to aggregated iron oxide nanoparticles only, that corresponds really to infinity) to 0.17 in order to tune the proportion of both particles into the aggregates, it was possible to tune the mean distance between iron oxide nanoparticles inside the aggregates. The value of 0.01 was arbitrary attributed to well dispersed iron oxide nanoparticles to gain into clarity on the log scale of Figure 5 (this corresponds to a mixing value of 0). SLP value of well dispersed IONPs was found to be 21.27 W/g at 7 mT and 335 kHz (red line in Figure 5).

When iron oxide nanoparticles only are aggregated, they exhibit a decreased value of the SLP down to 7 W/g at the same magnetic field and frequency. As aggregation induces a decrease of SLP, this result was almost achieved [4,23,24]. By tuning the iron oxide to cerium oxide ratio, we showed that the SLP values remained low for $r = 1.5$ (SLP value of 6.88 W/g). However, when the $r$ was decreased to 0.5, an increase of the SLP value was measured up to 11.7 W/g. This increase was confirmed when $r = 0.16$ (SLP value of 15.5 W/g). These results are explained by the fact that the iron oxide nanoparticles were "diluted" into the aggregates when $r$ was decreased, thus increasing the mean distance between magnetic nanoparticles. This dilution induced a decrease of dipolar interaction between nanoparticles, so that they could recover their ability to heat up their surrounding medium. The values of well dispersed nanoparticles were not reached for aggregates for two hypothetical reasons.

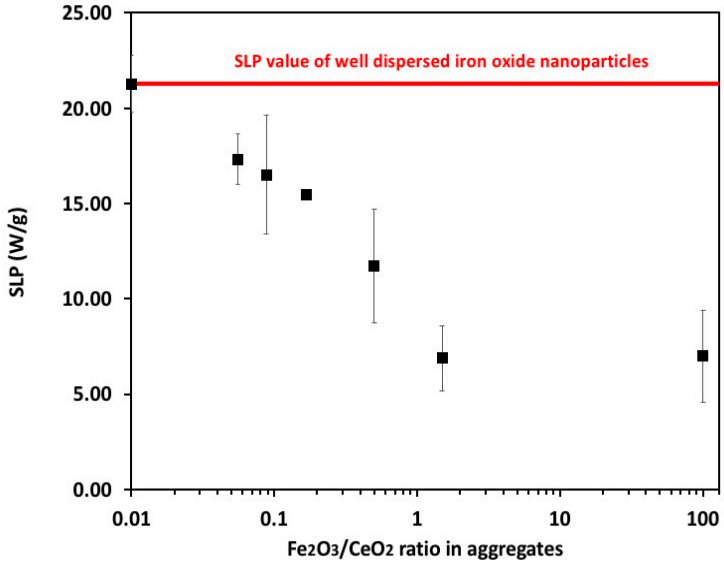


**Figure 5.** Specific loss power (SLP) versus the ratio between $Fe_2O_3/CeO_2$ ratio. Red line corresponds to the SLP of well dispersed IONPs. Error bars correspond to standard deviation of measurements of at least two samples.

First, particles in aggregates were too concentrated to avoid completely dipolar interactions. In a previous study, we established that iron oxide particles in similar aggregates were concentrated at a volume fraction of 20% [17]. For $r = 0.16$, this would correspond to a volume fraction around 3% (that correspond to 15% by weight), which is still a high concentration for the determination of SLP values for iron oxide nanoparticles [25]. As a comparison, SLP values of well dispersed iron oxide nanoparticles was determined at 0.67 wt % to avoid interparticle dipolar interactions.

Second, it could be still possible that the Brownian relaxation of iron oxide nanoparticles during hyperthermia was impeached when magnetic particles were located into the aggregates. However, the limit between Neel and Brownian relaxations for maghemite was found to be around 20 nm [26]. In our case, according to the size distribution (Figure 1), less than 1% of the particles had a diameter larger than 20 nm. Thus, all iron oxide particles behaved as superparamagnetic ones with a Neel relaxation ability. This argument is thus in favor of the first explanation.

## 4. Conclusions

In conclusion, we have measured the SLP values of iron oxide nanoparticles in aggregates containing various quantities of iron oxide and cerium oxide nanoparticles. As shown, aggregation of magnetic nanoparticles decreased the SLP values. The use of electrostatic bonds between both nanoparticles and oppositely charged polyelectrolytes allowed for the preparation of aggregates with homogeneous distributed iron oxide and cerium oxide nanoparticles. By diluting iron oxide nanoparticles in aggregates with cerium oxide nanoparticles, we were able to increase the SLP value back up to 79% of the SLP value of well-dispersed nanoparticles.

This model is of prime importance for designing materials with *a priori* stable magnetic properties toward new delivering systems for therapy applications. It would be of prime importance to look at different systems with directed linked (covalent bonds) or with more controlled architectures and their impact on hyperthermia efficiency.

**Author Contributions:** C.Y. prepared sample and achieved SLP measurements. A.M. performed TEM on cerium oxide and iron oxide nanoparticles. S.C. performed TEM on aggregates and the chemical mapping. J.F. conceptualized the experiments, analyzed the results, supervised the scientific discussions, and wrote the draft.

**Funding:** This research received no external funding.

**Conflicts of Interest:** The authors declare no conflict of interest.

## References


1. Di Corato, R.; Espinosa, A.; Lartigue, L.; Tharaud, M.; Chat, S.; Pellegrino, T.; Ménager, C.; Gazeau, F.; Wilhelm, C. Magnetic Hyperthermia Efficiency in the Cellular Environment for Different Nanoparticle Designs. *Biomaterials* **2014**, *35*, 6400–6411. [CrossRef] [PubMed]
2. Petri-Fink, A.; Steitz, B.; Finka, A.; Salaklang, J.; Hofmann, H. Effect of Cell Media on Polymer Coated Superparamagnetic Iron Oxide Nanoparticles (SPIONs): Colloidal stability, cytotoxicity, and cellular uptake studies. *Eur. J. Pharm. Biopharm.* **2008**, *68*, 129–137. [CrossRef] [PubMed]
3. Kolosnjaj-Tabi, J.; Javed, Y.; Lartigue, L.; Volatron, J.; Elgrabli, D.; Marangon, I.; Pugliese, G.; Caron, B.; Figuerola, A.; Luciani, N.; et al. The One Year Fate of Iron Oxide Coated Gold Nanoparticles in Mice. *ACS Nano* **2015**, *9*, 7925–7939. [CrossRef] [PubMed]
4. Guibert, C.; Dupuis, V.; Peyre, V.; Fresnais, J. Hyperthermia of Magnetic Nanoparticles: An Experimental Study of the Role of Aggregation. *J. Phys. Chem. C* **2015**, *119*, 28148–28154. [CrossRef]
5. Rosensweig, R.E. Heating Magnetic Fluid with Alternating Magnetic Field. *J. Magn. Magn. Mater.* **2002**, *252*, 370–374. [CrossRef]
6. Fortin, J.-P.; Wilhelm, C.; Servais, J.; Ménager, C.; Bacri, J.-C.; Gazeau, F. Size-Sorted Anionic Iron Oxide Nanomagnets as Colloidal Mediators for Magnetic Hyperthermia. *J. Am. Chem. Soc.* **2007**, *129*, 2628–2635. [CrossRef] [PubMed]
7. Hugounenq, P.; Levy, M.; Alloyeau, D.; Lartigue, L.; Dubois, E.; Cabuil, V.; Ricolleau, C.; Roux, S.; Wilhelm, C.; Gazeau, F.; et al. Iron Oxide Monocrystalline Nanoflowers for Highly Efficient Magnetic Hyperthermia. *J. Phys. Chem. C* **2012**, *116*, 15702–15712. [CrossRef]
8. Riedinger, A.; Guardia, P.; Curcio, A.; Garcia, M.A.; Cingolani, R.; Manna, L.; Pellegrino, T. Subnanometer Local Temperature Probing and Remotely Controlled Drug Release Based on Azo-Functionalized Iron Oxide Nanoparticles. *Nano Lett.* **2013**, *13*, 2399–2406. [CrossRef] [PubMed]
9. Dong, J.; Zink, J.I. Taking the Temperature of the Interiors of Magnetically Heated Nanoparticles. *ACS Nano* **2014**, *8*, 5199–5207. [CrossRef] [PubMed]
10. Griffete, N.; Fresnais, J.; Espinosa, A.; Wilhelm, C.; Bee, A.; Menager, C. Design of Magnetic Molecularly Imprinted Polymer Nanoparticles for Controlled Release of Doxorubicin under an Alternative Magnetic Field in Athermal Conditions. *Nanoscale* **2015**, *7*, 18891–18896. [CrossRef] [PubMed]
11. N'Guyen, T.T.T.; Duong, H.T.T.; Basuki, J.; Montembault, V.; Pascual, S.; Guibert, C.; Fresnais, J.; Boyer, C.; Whittaker, M.R.; Davis, T.P.; et al. Functional Iron Oxide Magnetic Nanoparticles with Hyperthermia-Induced Drug Release Ability by Using a Combination of Orthogonal Click Reactions. *Angew. Chem. Int. Ed.* **2013**, *52*, 14152–14156. [CrossRef]
12. Jolivet, J.P.; Massart, R.; Fruchart, J.M. Synthesis and Physicochemical Study of Non-Surfactant Magnetic Colloids in an Aqueous-Medium. *New J. Chem.* **1983**, *7*, 325–331.
13. Lefebure, S.; Dubois, E.; Cabuil, V.; Neveu, S.; Massart, R. Monodisperse Magnetic Nanoparticles: Preparation and Dispersion in Water and Oils. *J. Mater. Res.* **1998**, *13*, 2975–2981. [CrossRef]
14. Goharshadi, E.K.; Samiee, S.; Nancarrow, P. Fabrication of Cerium Oxide Nanoparticles: Characterization and Optical Properties. *J. Colloid Interface Sci.* **2011**, *356*, 473–480. [CrossRef] [PubMed]
15. Fresnais, J.; Yan, M.; Courtois, J.; Bostelmann, T.; Bée, A.; Berret, J.-F. Poly(Acrylic Acid)-Coated Iron Oxide Nanoparticles: Quantitative Evaluation of the Coating Properties and Applications for the Removal of a Pollutant Dye. *J. Colloid Interface Sci.* **2013**, *395*, 24–30. [CrossRef] [PubMed]
16. Jacquin, M.; Muller, P.; Lizarraga, G.; Bauer, C.; Cottet, H.; Théodoly, O. Characterization of Amphiphilic Diblock Copolymers Synthesized by MADIX Polymerization Process. *Macromolecules* **2007**, *40*, 2672–2682. [CrossRef]
17. Fresnais, J.; Berret, J.F.; Frka-Petesic, B.; Sandre, O.; Perzynski, R. Electrostatic Co-Assembly of Iron Oxide Nanoparticles and Polymers: Towards the Generation of Highly Persistent Superparamagnetic Nanorods. *Adv. Mater.* **2008**, *20*, 3877–3881. [CrossRef]
18. Yan, M.; Fresnais, J.; Berret, J.F. Growth Mechanism of Nanostructured Superparamagnetic Rods Obtained by Electrostatic Co-Assembly. *Soft Matter* **2010**, *6*, 1997–2005. [CrossRef]

19. Fresnais, J.; Lavelle, C.; Berret, J.F. Nanoparticle Aggregation Controlled by Desalting Kinetics. *J. Phys. Chem. C* **2009**, *113*, 16371–16379. [CrossRef]
20. Wildeboer, R.R.; Southern, P.; Pankhurst, Q.A. On the Reliable Measurement of Specific Absorption Rates and Intrinsic Loss Parameters in Magnetic Hyperthermia Materials. *J. Phys. D Appl. Phys.* **2014**, *47*, 495003. [CrossRef]
21. Chanteau, B.; Fresnais, J.; Berret, J.F. Electrosteric Enhanced Stability of Functional Sub-10 nm Cerium and Iron Oxide Particles in Cell Culture Medium. *Langmuir* **2009**, *25*, 9064–9070. [CrossRef] [PubMed]
22. Kanzaki, R.; Guibert, C.; Fresnais, J.; Peyre, V. Dispersion Mechanism of Polyacrylic Acid-Coated Nanoparticle in Protic Ionic Liquid, *N*,*N*-Diethylethanolammonium Trifluoromethanesulfonate. *J. Colloid Interface Sci.* **2018**. [CrossRef] [PubMed]
23. Cabrera, D.; Camarero, J.; Ortega, D.; Teran, F.J. Influence of the Aggregation, Concentration, and Viscosity on the Nanomagnetism of Iron Oxide Nanoparticle Colloids for Magnetic Hyperthermia. *J. Nanopart. Res.* **2015**, *17*. [CrossRef]
24. Landi, G.T. The Random Dipolar-Field Approximation for Systems of Interacting Magnetic Particles. *J. Appl. Phys.* **2013**, *113*, 163908. [CrossRef]
25. Branquinho, L.C.; Carrião, M.S.; Costa, A.S.; Zufelato, N.; Sousa, M.H.; Miotto, R.; Ivkov, R.; Bakuzis, A.F. Effect of Magnetic Dipolar Interactions on Nanoparticle Heating Efficiency: Implications for cancer hyperthermia. *Sci. Rep.* **2013**. [CrossRef] [PubMed]
26. Guibert, C.; Fresnais, J.; Peyre, V.; Dupuis, V. Magnetic Fluid Hyperthermia Probed by both Calorimetric and Dynamic Hysteresis Measurements. *J. Magn. Magn. Mater.* **2017**, *421*, 384–392. [CrossRef]


© 2018 by the authors. Licensee MDPI, Basel, Switzerland. This article is an open access article distributed under the terms and conditions of the Creative Commons Attribution (CC BY) license (http://creativecommons.org/licenses/by/4.0/).